Published in final edited form as:
J Cereb Blood Flow Metab. 2008 November ; 28(11): 1845–1859. doi:10.1038/jcbfm.2008.75.

Roscovitine reduces neuronal loss, glial activation and neurological deficits after brain trauma

Genell D. Hilton, Ph.D[*], **Bogdan A. Stoica, M.D.**[*,#], **Kimberly R. Byrnes, Ph.D.**, and **Alan I. Faden, M.D.**
Department of Neuroscience, Georgetown University Medical Center, Washington DC

Abstract

TBI causes both direct and delayed tissue damage. The latter is associated with secondary biochemical changes such as cell cycle activation that lead to neuronal death, inflammation and glial scarring. Flavopiridol — a CDK inhibitor that is neither specific nor selective — is neuroprotective. To examine the role of more specific CDK inhibitors as potential neuroprotective agents, we studied the effects of roscovitine in TBI. Central administration of roscovitine 30 minutes after injury resulted in significantly decreased lesion volume, as well as improved motor and cognitive recovery. Roscovitine attenuated neuronal death and inhibited activation of cell cycle pathways in neurons after TBI, as indicated by attenuated cyclin G1 accumulation and phosphorylation of retinoblastoma protein. Treatment also decreased microglial activation after TBI, as reflected by reductions in ED1, Galectin-3, $p22^{PHOX}$ and Iba-1 levels, and attenuated astrogliosis as shown by decreased GFAP accumulation. In primary cortical microglia and neuronal cultures, roscovitine and other selective CDK inhibitors attenuated neuronal cell death, as well as decreasing microglial activation and microglial-dependent neurotoxicity. These data support a multi-factorial neuroprotective effect of cell cycle inhibition after TBI-likely related to inhibition of neuronal apoptosis, microglial-induced inflammation and gliosis-and suggest that multiple CDKs are potentially involved in this process.

Keywords

cell cycle activation; microglia; neurons; roscovitine; TBI

Introduction

Traumatic brain injury (TBI) is a leading cause of morbidity and mortality in the children and adult population. In 2003 there were over 1.5 million TBI-related injuries in the United States resulting in approximately 1.2 million emergency room visits, 300,000 hospitalizations and 50,000 deaths. Annually, about 230,000 TBI survivors experience long-term disability from cognitive, emotional, sensory, motor and other impairments, making TBI a major public health problem.

In addition to causing direct mechanical injury, trauma initiates secondary cascades of biochemical and cellular changes that substantially contribute to subsequent tissue damage and related neurological deficits. Activation of specific signaling pathways in response to mechanical trauma causes delayed neuronal apoptosis as well as inflammation and reactive

[*]These authors contributed equally to this manuscript.
[#]Corresponding author: Bogdan A. Stoica, M.D., Georgetown University School of Medicine, Department of Neuroscience, Research Building, Room WG18, 3970 Reservoir Rd, NW, Washington, DC 20057, Office: 202.687.4609, Lab: 202.687.5172, Fax: 202.687.0617, email: stoicab@georgetown.edu

astrogliosis. Recent work has suggested a pathophysiological role for cell cycle pathways in neuronal apoptosis associated with both acute and chronic neurodegeneration. Post-mitotic cells such as neurons do not engage in cell cycle progression once they differentiate; thus, cell cycle proteins are generally down-regulated in these cells. However, mature neurons have the capacity to re-enter the cell cycle, a process that results in apoptosis rather than neuronal proliferation (Nguyen *et al* 2002). Abortive re-entry into the cell cycle has been shown to contribute to neuronal apoptosis *in vitro* and *in vivo*. Activation of cell cycle proteins has been implicated in *in vitro* neuronal cell death caused by excitotoxic stress, ceramide, β-amyloid, KCl withdrawal, trophic factor deprivation, and DNA damage of various etiologies (Kruman *et al* 2004). Cyclin-dependent kinases (CDKs) may also participate in neuronal apoptosis in the developing brain, as well as in neuronal degeneration in the adult brain following cerebral ischemia, Alzheimer's disease, Parkinson's disease, and amyotrophic lateral sclerosis (Nguyen *et al* 2003). Inhibition of cell cycle reactivation provides neuroprotection both *in vitro* and *in vivo* (Wang *et al* 2002). Previous studies in our laboratory have examined the role of cell cycle activation in the pathophysiology of experimental brain and spinal cord injury (SCI). Activation of the cell cycle occurs after TBI in both neurons and glial cells but with different downstream consequences: cellular proliferation/activation in astroglia and microglia cells *versus* apoptosis in neurons and oligodendroglial cells (Byrnes *et al* 2007). CNS injuries such as trauma and ischemia cause both proliferation of astroglia resulting in glial scar formation and microglial activation associated with release of pro-inflammatory molecules that contribute to neurotoxicity (Byrnes *et al* 2007). Although microglial activation may have protective actions in some experimental models, inhibition of brain inflammatory responses has proved neuroprotective in various models of neurodegeneration, as well as after neurotrauma (Byrnes *et al* 2006).

Progression through the cell cycle is controlled by the interaction of numerous cell cycle molecules including cyclins, CDKs and cyclin-dependent kinase inhibitors (CDKIs). Activation of these pathways, which regulate cell division in mitotic cells, causes cell death in mature neurons. Increased levels of G1 phase cyclins D and E associated with neuronal apoptosis have been demonstrated both in *in vitro* and *in vivo* models of excitotoxicity(Park *et al* 2000). Moreover, up-regulation of cyclins D, A, and B have been associated with toxin-induced hippocampal damage whereas increased protein levels of cyclin D1 and CDK4 appear to play a critical role in excitotoxin-induced neuronal cell death (Ino and Chiba 2001). Increased protein levels of cyclin D1 and CDK4 have been linked to the programmed cell death of motor neurons after spinal cord ischemia (Sakurai *et al* 2000). In rat fluid percussion TBI, injury significantly increases the expression of many cell cycle-related genes while down-regulating those of endogenous cell cycle inhibitors (Cernak *et al* 2005). Treatment with the powerful cell cycle inhibitor flavopiridol decreases TBI-induced lesion volume and improves behavioral outcomes following TBI (Cernak *et al* 2005), suggesting that modulation of the cell cycle following injury might provide a mechanism for neuroprotection. Unfortunatelly, flavopiridol is a relatively non-specific cell cycle inhibitor that also inhibits transcription, which complicates interpretation of its mechanism of action.

In the present studies we examined the effects of post-injury administration of the more specific cell cycle inhibitor roscovitine in a well-characterized rat TBI model. In parallel, we also examined the effects of roscovitine on microglial activation and microglial-dependent neurotoxicity using *in vitro* models.

Material and Methods

All protocols involving the use of animals complied with the Guide for the Care and Use of Laboratory Animals published by NIH (DHEW publication NIH 85-23-2985) and were approved by the Georgetown University Animal Use Committee.

Reagents

Roscovitine was obained from LC Laboratories (Woburn, MA); Purvalanol A (#540500), CDK1 inhibitor (#217695) and CDK4 inhibitor (#219477) were from Calbiochem (Gibbstown, NJ). Etoposide was from Tocris (Ellisville, Missouri)

Induction of Injury

Fluid percussion-induced TBI was performed as previously described (Yakovlev *et al* 1997) with some modifications. Briefly, male Sprague-Dawley rats (400±25 g) were housed in a 12 hour light, 12 hour dark cycle with free access to food and water. Rats were anesthetized with sodium pentobarbital (60mg/kg i.p.), followed by intubation and ventilation and implantation of a catheter in the tail artery to measure blood pressure. Temperature was measured rectally and maintained at 36-37° C throughout the procedure. A 5mm craniotomy over the left parietal cortex was placed midway between lambda and bregma and 3.9mm from the vertex and a metal female leur loc disc was cemented to the site. The other end of the attachment was then fitted to the fluid percussion device. Force of impact was controlled through a computer connected to the device through PowerLab (AD Instruments, Colorado Springs, CO, USA) and recorded through the Chart4Windows 4.2 software program (AD Instruments, Colorado Springs, CO). All rats were subjected to moderate injury (2.7 to 2.9 atm). Thirty minutes after injury, roscovitine (300nmoles of roscovitine in 10μl saline; this dose was chosen after pilot dose-response studies) or an equal volume vehicle (saline) was injected ICV contralateral to the injury site. Animals were sacrificed at 24 h or 7 days after injury (n=3-5 per group) for immunocytochemical/stereological studies, or at 21 days for histology, behavior and volumetric measurements (n=7-8 per group).

Neurologic Assessment

Motor and cognitive function was assessed post-injury using a composite neuroscore, as previously described (Cernak *et al* 2004), and the Morris water maze (MWM) as previously described (Faden *et al* 2003), respectively. Briefly, components of the composite neuroscore include measures of forelimb flexion (right and left), lateral pulsion (right and left), and the ability to maintain position on an angle board with animals positioned head up, head down, and right and left horizontal positions, each rated 0-5. For the MWM, rats were trained to locate a hidden, submerged platform using visual cues. The surface of the water was made opaque with the administration of white, nontoxic paint (Crayola) to the water. During training, the platform was maintained in a constant location in a single quadrant. The rat was placed in the water facing the wall at one of four randomly placed locations around the circular pool and the latency to find the hidden platform within 90 seconds was recorded. Trials were conducted on days 14, 15, 16 and 17 following injury. To control for motor impairment, rats were tested to locate a visible, elevated platform following the last training trial.

Microglial Cultures

Microglial cells were obtained from postnatal day 2 Sprague Dawley rat pups and cultured as described previously (Byrnes *et al* 2006).

Microglial Proliferation and Activation

Microglia were stimulated with lipopolysaccharide (LPS, 1μg/ml, Sigma, St. Louis, MO) with or without roscovitine (100 μM) pre-treatment (60 min). Microglial proliferation was then assessed using the MTS assay (Promega, Madison, WI) according to the manufacturer's protocols. Microglia activation reflected by Nitric Oxide (NO) production was assayed using the Griess Reagent Assay (Invitrogen, Carlsbad, CA), according to the manufacturer's instructions.

Microglia-Induced Neurotoxicity

Rat primary cortical neuronal cultures were derived from E18 Sprague Dawley rat cortices (Taconic, Germantown, NY) as previously described (Mukhin *et al* 1998). At day 7 *in vitro*, media from microglia that had been stimulated with LPS with or without roscovitine pre-treatment was transferred to the neuronal cultures. At 24 h after incubation with microglial-conditioned media, the LDH release assay (CytoTox 96® Nonradioactive Cytotoxicity Assay Kit, Promega, Madison, WI) was used to assess neuronal cell death.

Etoposide-Induced Neuronal cell death

For etoposide-induced neuronal cell death, primary neurons were pretreated with the various CDK inhibitors (roscovitine 25μM, 50μM, 100μM; purvanalol A 25μM, 50μM; CDK1 inhibitor 25μM, 50μM, 100μM; and CDK4 inhibitor 25μM, 50μM) followed by exposure to etoposide (50μM). After 24 h neuronal cell death was determined using the LDH assay as described.

Immunocytochemistry/Stereology

At 24 h and 7 days after injury, animals were sacrificed and brains harvested for histopathological analyses as described (Di Giovanni *et al* 2005). Brains were frozen-sliced on a cryostat at a thickness of 20μm, collected at a 1:5 ratio. Selected slides from animals at 24 h after injury were stained with Fluoro-Jade C (Chemicon, Temecula, CA) to identify degenerating neurons following the manufacturer's instructions.

For immunocytochemistry, sections were processed as previously described (Byrnes *et al* 2007) using one or more antibodies recognizing the following targets: markers of cell cycle activation including Cyclin G1 (sc-7865, 1:50, Santa Cruz Biotechnology, Santa Cruz, CA), and phospho S780 retinoblastoma (Rb) protein (ab47763, 1:100, Abcam, Cambridge, MA); markers of microglial activation such as CD68 (clone ED1, MCA341R, 1:100, Serotec, Raleigh, NC), Galectin-3 (ab2785, 6μl/ml, Abcam), $p22^{PHOX}$ (sc-20781, 1:50, Santa Cruz Biotechnology); the neuronal marker NeuN protein (clone A60, MAB37 at 1:100, Chemicon, Billerica, MA) and the astroglia marker GFAP (MAB360, 1:400, Chemicon). The fluorescence microscopy imaging was performed using Zeiss 510 Meta confocal laser scanning microscope (LSM 510 META, Thornwood, NY) as previously described (Byrnes *et al* 2007). The images were taken using the 10X objective at 1024×1024 resolution covering a field of view of 921.36μm × 921.36μm; all images in the same series, including sham, vehicle and roscovitine using the same antibodies were aquired using the same instrument parameters. By using the multi-tile image acquisition capabilities of Zeiss LSM 510 META with a motorized stage, 16 images were taken of adjacent areas of the brain. These images were automatically spliced together to create a final image having an 3685.45 μm × 3685.45 μm field of view at a resolution of 4096×4096 pixels. Modest variations in image brightness between adjacent panels of the composite image are intrinsic to this method.

Automatic cell counting in multi-tile fluorescent images obtained as described above was performed using the ImageJ software, version 1.4 (National Institutes of Health). The indicated number of images, obtained from independent sections and including the channel of interest were first converted to 8-bit grayscale using the Image>Type command. Next, the background was set as indicated using the Image>Adjust>Threshold command followed by cell analysis including cell counting using the Analyze>Analyze Particles command. All images in the same series, including vehicle and roscovitine using the same antibodies were processed using the same analysis parameters and the entire image was used for counting. The numbers shown in the graphs represent the average number of cells per image for each treatment. Unlike stereology which offers a quantitative assesment of the total cell number throughout the entire lesion volume, this method provides a semi-quantitative representation of cell number per

representative field (the multi-tiled images presented) of 3-5 sections. Detailed instructions are available at: http://rsbweb.nih.gov/ij/docs/menus/analyze.html.

Unbiased stereology, using the Stereologer 2000 program (SRC, Chester, MD), was applied for quantitation after standard immunohistochemistry (IHC) staining as previously described (Byrnes *et al* 2007). The multi-level sampling design in the Stereologer 2000 software, based upon the fractionator sampling method, was used to estimate the cell numbers of a particular phenotype in the injured hemisphere. For cyclin G1 cell counting purposes, the area of injury was outlined using a 1.5x objective, and cells within each area were counted using a 40X objective. For phospho Rb cell counting purposes, the area immediately adjacent to the site of injury was outlined as described above.

Histology

At 21 days following injury, animals were decapitated and tissue processed as above. Slices were stained with Gill's hematoxylin, followed by counterstaining in 2.5% eosin and cover-slipped. Lesion volume was measured based on the Cavalieri method of stereology and performed on tissue obtained 21 days following injury, as previously described (Byrnes *et al* 2007). The lesion area, including both the cavity and surrounding damaged tissue, was outlined using the Stereologer 2000 program to obtain final volume measurements.

Statistics

Continuous variables subjected to repeated measures over a period of time (MWM) were analyzed using repeated measures ANOVA followed by a one-way at each time point ($P<0.05$). *T*-test and one-way ANOVA were performed for stereologic analysis with significance set at $P<0.05$. All continuous data are shown as mean ± SEM. Ordinal measurements (composite neuroscore) were evaluated using the Kruskal-Wallis test with individual Mann-Whitney U tests corrected for multiple comparisons. Statistical significance was set at $P<0.05$.

Results

Roscovitine reduces lesion volume and improves behavioral outcomes following TBI

As shown in Fig. 1, stereological analysis of lesion volume at 21 days following TBI indicated that treatment with roscovitine decreased brain lesion volume by 37% compared to vehicle-treated animals ($t= 5.073$, $P<0.001$). The average vehicle-treated lesion volume was 20.6 mm^3 and the average roscovitine-treated lesion volume was 13.0 mm^3. Roscovitine treatment also significantly improved composite neuroscores compared to vehicle-treated animals at 14 and 21 days following injury (Kruskal Wallis 8.346; $P<0.02$; Fig. 2A). Individual Mann-Whitney U tests, corrected for multiple measurements, revealed that vehicle-treated injured animals achieved significantly lower neuroscores compared to sham ($P<0.005$), and that roscovitine improved motor outcome compared to vehicle at both 14 ($P<0.02$) and 21 days ($P<0.001$) post-injury.

Analysis of cognitive function following injury showed a significant effect of time ($F_{3,51} = 24.32$; $P<0.0001$) and treatment ($F_{2,51} = 7.48$; $P<0.005$; Fig. 2B). Latency to platform in the MWM test in vehicle-treated injured rats was significantly longer on days 16 and 17 post-injury ($P<0.05$ and $P<0.001$, respectivelly), compared to sham-injured animals. However, there was no significant difference in performance between sham- and roscovitine-treated animals on day 16, suggesting that roscovitine induced improvement in cognitive function. By day 17 post-injury, cognitive performance in roscovitine-treated injured animals was improved compared to vehicle-treated injured animals ($P<0.05$).

Roscovitine decreases neuronal cell death after TBI

To explore the effects of roscovitine on neuronal survival we performed Fluoro-Jade C staining after TBI. Fluoro-Jade C specifically stains dying neurons, which become fluorescent green. As shown in Fig. 3A, tissue obtained 24 h post-injury revealed Fluoro-Jade C-labeled degenerating neurons at the site of cortical injury lesion in vehicle-treated animals. Animals treated with roscovitine appeared to have a smaller injury lesion that contained fewer Fluoro-Jade C positive cells. No significant Fluoro Jade C staining was visible in sham animals (data not shown). We used the analysis capabilities of the ImageJ software to count Fluoro-Jade-positive cells in several independent sections such as the one presented, from vehicle and roscovitine treated animals exposed to TBI; there is a significant decrease in Fluoro-Jade-positive cells in sections from roscovitine treated animals (Fig. 3B).

Roscovitine significantly attenuates the numbers of neurons positive for markers of cell cycle activation

In order to explore the mechanisms responsible for the roscovitine-induced neuroprotective effects, we examined two markers of cell cycle activation, Cyclin G1 and phosphorylated Rb, which we have previously shown to increase in apoptotic neurons following SCI (Di Giovanni *et al* 2003). Staining with NeuN, a DNA-binding neuron specific protein was used to confirm the presence of cell cycle markers in neurons. Immunocytochemical analysis revealed that at 24 h after injury, in vehicle-treated animals, there is an increased expression of cyclin G1 within the more central area of the lesion site (Fig. 4A) while phosphorylated Rb was relatively more present on the periphery of the injury (Fig. 5A). Both markers co-localized with the NeuN immunostaining, indicating that cell cycle activation occurred in neurons. This eleveted expression of cyclin G1 and Rb phosphorylation was reduced in tissue from animals treated with roscovitine (Figs. 4A and 5A) suggesting that the neuroprotective effect of this specific CDKs inhibitor is associated with down-regulation of cell cycle pathways. We performed cell counting on several independent sections such as the one presented, using the ImageJ software; roscovitine treatment results in a significant decrease in the number of cyclin G1 and Phospho-Rb, Fig. 4B and Fig. 5B respectivelly. No significant cyclin G1 or phospho-Rb immunostaining was detected in sham animals (data not shown).

In order to obtain a true quantitative assessment of the differences in Cyclin G1 and phosphorylated Rb between vehicle- and roscovitine-treated animals, stereological analysis was performed at 24 h post-injury. Injury induced a large increase in both cyclin G1 expression ($F_{2,9} = 7.299$, $P<0.02$; Fig. 4C) and phosphorylation of Rb ($F_{2,10} = 27.386$; $P<0.001$; Fig. 5C) compared to sham. Similar trends are observed with the two methods of cell counting, the semi-quantitative analysis of immunofluorescent images and quantitative stereology.

Roscovitine decreases activation of astrocytes and microglia after TBI

In order to examine the effects of TBI and cell cycle inhibition on astroglia and microglial activation, animals were treated with either vehicle or roscovitine after injury and sacrificed 7 days later. In vehicle-treated animals, TBI increased the number of activated astroglia as evidenced by intensified staining for glial fibrillary acidic protein (GFAP), an indicator of astrocyte reactive response to CNS injury (Brenner 1994).

Injury also resulted in activation of microglia as indicated by increased staining with four separate microglia markers - $p22^{PHOX}$, Galectin-3, ED1 and Iba-1. $p22^{PHOX}$ is a critical component of the microglia NADPH Oxidase complex (DeLeo and Quinn 1996), responsible for reactive oxygen species (ROS) generation and involved in microglia proliferation/activation (Byrnes *et al* 2006). The activated microglia indicated by $p22^{PHOX}$ infiltrated the core of the lesion site whereas activated astroglia appeared to surround the lesion site. (Fig. 6A). In contrast, animals treated with roscovitine showed decreased expression of both GFAP-

positive astroglia as well as $p22^{PHOX}$ positive microglia (Fig. 6A), suggesting that cell cycle inhibition attenuates both astrocyte activation and microglial activation associated with brain injury. Cell counting on several similar sections using the ImageJ program shows the significant decrease in the numbers of GFAP and $p22^{PHOX}$-positive cells following roscovitine treatment (Fig. 6A).

In vehicle-treated animals, TBI induced an increase in the number of activated microglia as evidenced by staining for ED1, a lysosomal membrane glycoprotein that is a marker of microglial phagocytic activation (Damoiseaux *et al* 1994) (Fig. 6B). The ED1-positive microglia are not co-stained with Cyclin G1, suggesting that induction of this cell cycle protein is not involved in microglia activation. Animals treated with roscovitine showed decreased expression of ED1 positive microglia, suggesting that cell cycle inhibition attenuates microglial activation associated with injury. Cell counting on similar sections using the ImageJ program shows a significant decrease in the number of ED1-positive cells following roscovitine treatment (Fig. 6B). The presence of activated microglia in the lesion site after TBI was also confirmed by immunostaining for Galectin-3 (MAC-2 antigen, a beta-galactoside-specific lectin), which is selectively expressed by activated microglia in the brain (Walther *et al* 2000). In vehicle-treated animals, TBI increased the number of microglia with intense Galectin-3 staining in the injury core (Fig. 6C). Animals treated with roscovitine showed a marked decrease in Galectin-3-positive microglia, suggesting that cell cycle inhibition attenuates microglia activation associated with brain injury. Cell counting on similar sections using the ImageJ program demonstrates a significant decrease in the numbers of Galectin-3-positive cells following roscovitine treatment (Fig. 6C). Finally, microglia activation was also confirmed by immunostaining for Iba-1, which is a calcium-binding protein that is specifically expressed in brain microglia and upregulated upon microglia activation (Ito *et al* 2001). In vehicle-treated animals, TBI increased the number of microglia with strong Iba-1 staining in the injury core (Fig. 6D). Animals treated with roscovitine showed a marked decrease in Iba-1-positive microglia, further confirming that cell cycle inhibition attenuates microglial activation associated with brain injury. Cell counting on similar sections using the ImageJ program demonstrated a significant decrease in the numbers of Iba-1-positive cells following roscovitine treatment (Fig. 6D). No significant cyclin G1, Galectin-3, $p22^{PHOX}$ or GFAP immunostaining was detected in sham animals (data not shown).

Roscovitine decreases activation of primary microglia in in vitro culture models

To further investigate the potential of roscovitine to attenuate microglial activation, we used an *in vitro* culture system based on primary rat brain microglia stimulated by lipopolysacharide (LPS). Pre-treatment with roscovitine significantly attenuated markers of microglial activation such as proliferation (Fig. 7A) and release of NO, a well known neurotoxic agent (Fig. 7B). In this model we also examined other CDK inhibitors with relatively narrow specificities, including a CDK1-selective inhibitor and a CDK4-selective inhibitor. The CDK1 inhibitor is approximatelly 5 times more selective for CDK1 compared to CDK5 (Andreani *et al* 2000). The CDK4 inhibitor is 500 times more selective for CDK4 compared to CDK2 (Kubo *et al* 1999). Pre-treatment with both CDK1 and CDK4 inhibitors significantly attenuated both microglial proliferation (Fig. 7C) and release of NO (Fig. 7D).

We used an *in vitro* model of mixed primary brain microglia-neuronal cultures to evaluate the potential of roscovitine to attenuate microglial-dependent neurotoxicity. Pre-treatment of microglia with roscovitine before LPS treatment for 24 h significantly attenuated the ability of microglial conditioned media to induce neuronal cell death (Fig. 7E). These data suggest that roscovitine decreases release of neurotoxic compounds by activated microglia.

Finally, we examined the effects of roscovitine as well as other CDK inibitors in a well established model of neuronal apoptosis induced by etoposide. In addition to roscovitine,

CDK1 and CDK4 inhibitors, we also used Purvalanol A, a compound that has a CDK inhibitory profile similar to roscovitine and may be used to confirm roscovitine-based data indicating the involvement of CDKs in a process (Bain *et al* 2007). As shown in Fig.7F, all of the tested CDKs inhibitors were able to significantly attenuate etoposide-induced neuronal cell death, suggesting the involvement of multiple CDKs in neuronal apoptosis.

Discussion

Over the past several years our group has studied the role of cell cycle activation in the pathophysiology of CNS trauma. After SCI (Byrnes and Faden 2007; Di Giovanni *et al* 2003) or TBI (Cernak *et al* 2005) in rats, increased expression of cell cycle proteins occurred in neurons showing caspase-3 activation and morphological signs of apoptosis. Cell cycle activation after TBI was also associated with astrogliosis and microglial activation (Di Giovanni *et al* 2005). Treatment with flavopiridol reduced behavioral and histological abnormalities after TBI (Di Giovanni *et al* 2005) and SCI (Byrnes *et al* 2007). Protective effects of flavopiridol have also been reported in cerebral ischemia (Wang *et al* 2002).

Flavopiridol, a semi-synthetic flavonoid, is a potent but non-selective competitive CDK inhibitor acting on all CDKs thus far examined (Newcomb 2004). Unfortunately, it also potently inhibits the positive transcription elongation factor b (P-TEFb, of which CDK9 is a component) and consequently acts as a global suppressor of transcription (Monaco *et al* 2004). In contrast, roscovitine is a purine analogue that competitively inhibits CDKs in a more selective fashion, acting preferentially on CDK 1, 2, and 5 and possibly CDK7 and 9 (Meijer *et al* 1997). It poorly inhibits CDK4 and 6 (Meijer *et al* 1997) and does not significantly inhibit members of most other kinase families (Bain *et al* 2003). Overall, multiple studies have confirmed that roscovitine is among the most potent and specific CDK inhibitors (Bach *et al* 2005; Bain *et al* 2007; Meijer *et al* 1997). Moreover, although roscovitine can inhibit CDK9 *in vitro*, it does not appear to interact with it *in vivo*; this may explain why, unlike flavopiridol, roscovitine does not globally inhibit gene expression (Lam *et al* 2001). Because both RNA and protein synthesis may be required for induction of neuronal apoptosis, it is likely that the ability of flavopiridol to attenuate neuronal cell death reflects in part to its transcriptional repressor role. Therefore, to better address whether activation of CDKs/cell cycle activation is an important mechanism for TBI-induced cellular changes and related functional deficits, we examined the effect of roscovitine treatment.

Central administration of a single dose of roscovitine 30 min after injury markedly decreased lesion volume and significantly improved behavioral outcomes compared to vehicle-treated animals. Quantitative stereological techniques and high resolution confocal microscopy were used to characterize the molecular and cellular changes induced by TBI and its modulation by roscovitine. Following TBI, activation of neuronal cell cycle pathways—including phosphorylation of Rb protein and increased expression of cyclin G1—as well as neuronal cell death occur within 24 h; considerable microglial and astrocyte activation/proliferation were detected by 7 days. Roscovitine treatment significantly attenuated each of these changes. At 24 h, roscovitine-treated animals showed decreased numbers of neurons positive for phosphorylated-Rb and cyclin G1 as compared to controls and fewer degenerating neurons indicated by decreased Fluoro-Jade C staining. At 7 days post-injury, roscovitine treatment reduced microglial activation as demonstrated by reduced numbers of cells positive for ED1, Galectin-3 and $p22^{PHOX}$, and decreased astrocyte activation as indicated by fewer GFAP-positive cells. Decreased numbers of cyclin G1-positive cells were also found at this later time point, suggesting that roscovitine-induced inhibition of cell cycle activation after a single early injection is sustained.

The mechanisms by which the active cyclins/CDKs complexes induce neuronal apoptosis are being clarified. One of the signal transduction pathways involved includes cyclin D-dependent CDK4/6 which phosphorylates Rb on specific residues. Phosphorylation of Rb causes dissociation of Rb from the Rb/E2Fs complex, with activation of E2Fs transcription factors; E2Fs induce apoptosis by upregulating cell death mechanisms such as activation of B- and C-myb genes; by increasing expression of caspases 3, 9 and 8 and Apaf-1; and through activation of p53 and p73. These activities lead to increased expression of pro-apoptotic Bcl-2 family members and release of mitochondrial pro-apoptotic proteins (Nguyen *et al* 2003). Recent reports indicate that in some models of neuronal cell death activation of CDK5 is upstream of CDK4/6 and that CDK5 can directly phosphorylate Rb and initiate neuronal cell death (Hamdane *et al* 2005). CDK5 is implicated in neurodegeneration and cell death; knockout of CDK5 results in neuroprotection after focal brain ischemia (Rashidian *et al* 2005). CDK2 can also phosphorylate Rb (Lundberg and Weinberg 1998). As roscovitine has no activity against CDK4 and CDK6, but is highly potent against CDK2 and CDK5 (Meijer and Raymond 2003), our data suggest that activation of CDK2 and/or CDK5 may contribute to neuronal cell death after TBI and that roscovitine might downregulate Rb phosphorylation by inhibiting CDK2/5. It is important to underscore that specificity limitations common to pharmacological interventions, such as the one used in our study, do not allow a determination of the precise CDK that is targeted by roscovitine and is responsible for the protective effects observed. Furthermore, our data do not exclude the possibility that other CDKs besides CDK2 or CDK5 are involved in neuronal cell death or other cellular processes that are active in our model. As discussed above, multiple CDKs are often involved in sequential and/or parallel activation cascades when modulating cellular activity. Therefore, treatment effects may result from interventions at multiple points in the reaction cascade. Our *in vitro* data are consistent with this conclusion, showing that in addition to roscovitine and purvalanol A, which target multiple CDKs, etoposide-induced neuronal cell death and/or primary microglial activation in culture are also attenuated by somewhat selective CDK1 and CDK4 inhibitors. In addition, published reports indicate that significant redundancy exists in CDK signaling. For example, CDK2 knockout mice are viable and show no significant proliferation effects, despite previous data indicating an important function for CDK2 in the cell cycle; this suggests that other CDKs may be able to compensate for the loss of CDK2 (Berthet *et al* 2003). Thus, targeting multiple CDKs may provide better neuroprotection than more selective inhibitors.

A role for increased Cyclin G1 expression and Rb phosphorylation in neuronal cell death has also been suggested in other experimental models, including ischemia, excitotoxicity, and neurodegeneration (Sultana and Butterfield 2007). Cyclin G1 immunoreactivity and mRNA are low in mature rodent brain; however, following injury, expression increases in the nuclei of damaged neurons. Cyclin G1 positive neurons also correlate strongly with degenerating neurons in a model of permanent middle cerebral artery occlusion (MCAO) (Maeda *et al* 2005).

Phosphorylated Rb induced by hypoxia-ischemia and MCAO is expressed in pyknotic cells and neurons both in the injury core and peri-infarct regions (Rashidian *et al* 2005). In our model, Cyclin G1 was expressed preferentially, albeit not exclusively, in neurons in the central area of the lesion, whereas phosphorylated Rb was expressed relatively more in the neurons toward the periphery of the injury lesion. This might suggest differential activation of cell cycle components in the central lesion area *versus* penumbra, although variations in the time course of cell cycle activation may provide an alternative explanation.

Cyclin G1 over-expression induces cell death (Okamoto *et al* 1999), although the mechanisms responsible for cyclin G1 induction following injury and related neuronal cell death are not well characterized. Some recent data suggest that cyclin G1 is a target gene of the p53 tumor suppressor protein, a well-known inducer of apoptotic cell death. In this case, cyclin G1 would

be downstream of the signaling pathway involving phosphorylation of Rb and activation of E2Fs transcription factors that lead to p53 activation. Other data indicate that Cyclin G1 is associated with CDK5 and plays a role in G2/M transition (Seo *et al* 2006); under these conditions increased activation of cyclin G1 may induce apoptosis of mature neurons that are unable to divide.

While CNS injury-induced aberrant cell cycle activation induces apoptosis in post-mitotic cells, it initiates proliferation in mitotic CNS resident cells such as astrocytes and microglia (Takuma *et al* 2004). The functional significance of microglial proliferation and microglial activation has been debated. On the one hand, activated microglia produce various pro-inflammatory molecules, such as IL-1β, NO, complement components, MCP-1, osteopontin, MHC class I and II and ROS (produced by the NADPH oxidase enzyme) and these have been implicated in secondary injury (Cernak *et al* 2005). On the other hand, microglial-related factors such as TNFα may participate in both secondary injury and recovery (Tamatani *et al* 1999), whereas others such GDNF may provide endogenous neuroprotection (Hashimoto *et al* 2005). Similarly, although astrocytes play an important role in maintaining normal brain function, changes after injury such as swelling and/or hypertrophy (astrogliosis) as well as proliferation (astrocytosis) may serve pathophysiological actions (Cernak *et al* 2005). For example, the glial scar associated with astrocytosis may inhibit regeneration and plasticity after brain injury (Silver and Miller 2004). A recent *in vitro* study of ischemia has suggested that the neurotoxic versus neuroprotective actions of activated microglia may in part reflect injury severity (Lai and Todd 2008).

We have shown previously that cell cycle proteins are up-regulated in microglia after SCI as well as in primary microglia *in vitro* (Byrnes *et al* 2006) and that activation of astrocytes and microglia occur after SCI and are correlated with cell cycle initiation (Byrnes *et al* 2007). Another group has reported cell cycle activation in microglia after SCI and protective actions by the cell cycle inhibitor olomoucine (Tian *et al* 2007). We established with a high degree of confidence the post-injury microglia status in the brain by using four independent markers of microglia activation: ED1, Galectin-3, $p22^{PHOX}$ and Iba-1 (Byrnes *et al* 2006; Ito *et al* 2001). The present studies demonstrate that microglial activation occurs after TBI, as indicated by the greatly increased number of cells positive for the three markers. These changes are attenuated by roscovitine. Roscovitine treatment also inhibited TBI-induced activation of astrocytes as shown by decreased staining with GFAP-marker of astrocyte reactive response (Brenner 1994). Because the complex cellular environment in the brain makes it difficult to determine with precision the primary action of any pharmacological agent, we used cell culture models of primary microglia and neurons to analyze the effects of roscovitine on specific cell types. In previous *in vitro* studies we have demonstrated that roscovitine is protective against neuronal cell death resulting from etoposide-induced DNA damage and also that roscovitine inhibits astrocyte proliferation (Cernak *et al* 2005). In the present study we focused on the effects of roscovitine on primary microglia using a well established model of LPS-induced activation. In this model, roscovitine attenuated microglial proliferation and the release of neurotoxic molecules such as NO induced by LPS. Furthermore, using a model of mixed primary microglia/neuronal cultures, we show that roscovitine markedly reduced microglial-dependent neurotoxicity. CDK1 and CDK4 inhibitors also attenuate microglia activation in our *in vitro* model, suggesting complexity of the CDK cascade that regulates microglia functions.

In conclusion, roscovitine treatment after TBI markedly reduces lesion volume and improves behavioral outcome. Treatment attenuates cell cycle activation in neurons, astrocytes and microglia; effects are associated with reductions in neuronal apoptosis, glial scar formation and microglial activation. These diverse effects of roscovitine are supported by complementary cell culture observations, and such pluripotential actions may explain its robust neuroprotective activity.

Acknowledgments

Support: National Institutes of Health (NS052568 to AIF)

References

Andreani A, Cavalli A, Granaiola M, Leoni A, Locatelli A, Morigi R, Rambaldi M, Recanatini M, Garnier M, Meijer L. Imidazo[2,1 -b]thiazolylmethylene- and indolylmethylene-2-indolinones: a new class of cyclin-dependent kinase inhibitors. Design, synthesis, and CDK1/cyclin B inhibition. Anticancer Drug Des 2000;15:447–52. [PubMed: 11716438]

Bach S, Knockaert M, Reinhardt J, Lozach O, Schmitt S, Baratte B, Koken M, Coburn SP, Tang L, Jiang T, Liang DC, Galons H, Dierick JF, Pinna LA, Meggio F, Totzke F, Schachtele C, Lerman AS, Carnero A, Wan Y, Gray N, Meijer L. Roscovitine targets, protein kinases and pyridoxal kinase. J Biol Chem 2005;280:31208–19. [PubMed: 15975926]

Bain J, McLauchlan H, Elliott M, Cohen P. The specificities of protein kinase inhibitors: an update. Biochem J 2003;371:199–204. [PubMed: 12534346]

Bain J, Plater L, Elliott M, Shpiro N, Hastie CJ, McLauchlan H, Klevernic I, Arthur JS, Alessi DR, Cohen P. The selectivity of protein kinase inhibitors: a further update. Biochem J 2007;408:297–315. [PubMed: 17850214]

Berthet C, Aleem E, Coppola V, Tessarollo L, Kaldis P. Cdk2 knockout mice are viable. Curr Biol 2003;13:1775–85. [PubMed: 14561402]

Brenner M. Structure and transcriptional regulation of the GFAP gene. Brain Pathol 1994;4:245–57. [PubMed: 7952266]

Byrnes KR, Garay J, Di Giovanni S, De Biase A, Knoblach SM, Hoffman EP, Movsesyan V, Faden AI. Expression of two temporally distinct microglia-related gene clusters after spinal cord injury. Glia 2006;53:420–33. [PubMed: 16345062]

Byrnes KR, Faden AI. Role of Cell Cycle Proteins in CNS Injury. Neurochem Res. 2007

Byrnes KR, Stoica BA, Fricke S, Di Giovanni S, Faden AI. Cell cycle activation contributes to post-mitotic cell death and secondary damage after spinal cord injury. Brain 2007;130:2977–92. [PubMed: 17690131]

Cernak I, Vink R, Zapple DN, Cruz MI, Ahmed F, Chang T, Fricke ST, Faden AI. The pathobiology of moderate diffuse traumatic brain injury as identified using a new experimental model of injury in rats. Neurobiol Dis 2004;17:29–43. [PubMed: 15350963]

Cernak I, Stoica B, Byrnes KR, Di Giovanni S, Faden AI. Role of the cell cycle in the pathobiology of central nervous system trauma. Cell Cycle 2005;4:1286–93. [PubMed: 16082214]

Damoiseaux JG, Dopp EA, Calame W, Chao D, MacPherson GG, Dijkstra CD. Rat macrophage lysosomal membrane antigen recognized by monoclonal antibody ED1. Immunology 1994;83:140–7. [PubMed: 7821959]

DeLeo FR, Quinn MT. Assembly of the phagocyte NADPH oxidase: molecular interaction of oxidase proteins. J Leukoc Biol 1996;60:677–91. [PubMed: 8975869]

Di Giovanni S, Knoblach SM, Brandoli C, Aden SA, Hoffman EP, Faden AI. Gene profiling in spinal cord injury shows role of cell cycle in neuronal death. Ann Neurol 2003;53:454–68. [PubMed: 12666113]

Di Giovanni S, Movsesyan V, Ahmed F, Cernak I, Schinelli S, Stoica B, Faden AI. Cell cycle inhibition provides neuroprotection and reduces glial proliferation and scar formation after traumatic brain injury. Proc Natl Acad Sci U S A 2005;102:8333–8. [PubMed: 15923260]

Faden AI, Knoblach SM, Cernak I, Fan L, Vink R, Araldi GL, Fricke ST, Roth BL, Kozikowski AP. Novel diketopiperazine enhances motor and cognitive recovery after traumatic brain injury in rats and shows neuroprotection in vitro and in vivo. J Cereb Blood Flow Metab 2003;23:342–54. [PubMed: 12621309]

Hamdane M, Bretteville A, Sambo AV, Schindowski K, Begard S, Delacourte A, Bertrand P, Buee L. p25/Cdk5-mediated retinoblastoma phosphorylation is an early event in neuronal cell death. J Cell Sci 2005;118:1291–8. [PubMed: 15741232]

Hashimoto M, Nitta A, Fukumitsu H, Nomoto H, Shen L, Furukawa S. Inflammation-induced GDNF improves locomotor function after spinal cord injury. Neuroreport 2005;16:99–102. [PubMed: 15671854]

Ino H, Chiba T. Cyclin-dependent kinase 4 and cyclin D1 are required for excitotoxin-induced neuronal cell death in vivo. J Neurosci 2001;21:6086–94. [PubMed: 11487632]

Ito D, Tanaka K, Suzuki S, Dembo T, Fukuuchi Y. Enhanced expression of Iba1, ionized calcium-binding adapter molecule 1, after transient focal cerebral ischemia in rat brain. Stroke 2001;32:1208–15. [PubMed: 11340235]

Kruman II, Wersto RP, Cardozo-Pelaez F, Smilenov L, Chan SL, Chrest FJ, Emokpae R Jr. Gorospe M, Mattson MP. Cell cycle activation linked to neuronal cell death initiated by DNA damage. Neuron 2004;41:549–61. [PubMed: 14980204]

Kubo A, Nakagawa K, Varma RK, Conrad NK, Cheng JQ, Lee WC, Testa JR, Johnson BE, Kaye FJ, Kelley MJ. The p16 status of tumor cell lines identifies small molecule inhibitors specific for cyclin-dependent kinase 4. Clin Cancer Res 1999;5:4279–86. [PubMed: 10632371]

Lai AY, Todd KG. Differential regulation of trophic and proinflammatory microglial effectors is dependent on severity of neuronal injury. Glia 2008;56:259–70. [PubMed: 18069670]

Lam LT, Pickeral OK, Peng AC, Rosenwald A, Hurt EM, Giltnane JM, Averett LM, Zhao H, Davis RE, Sathyamoorthy M, Wahl LM, Harris ED, Mikovits JA, Monks AP, Hollingshead MG, Sausville EA, Staudt LM. Genomic-scale measurement of mRNA turnover and the mechanisms of action of the anti-cancer drug flavopiridol. Genome Biol 2001;2RESEARCH0041

Lundberg AS, Weinberg RA. Functional inactivation of the retinoblastoma protein requires sequential modification by at least two distinct cyclin-cdk complexes. Mol Cell Biol 1998;18:753–61. [PubMed: 9447971]

Maeda M, Ampo K, Kiryu-Seo S, Konishi H, Ohba N, Kadono C, Kiyama H. The p53-independent nuclear translocation of cyclin G1 in degenerating neurons by ischemic and traumatic insults. Exp Neurol 2005;193:350–60. [PubMed: 15869937]

Meijer L, Borgne A, Mulner O, Chong JP, Blow JJ, Inagaki N, Inagaki M, Delcros JG, Moulinoux JP. Biochemical and cellular effects of roscovitine, a potent and selective inhibitor of the cyclin-dependent kinases cdc2, cdk2 and cdk5. Eur J Biochem 1997;243:527–36. [PubMed: 9030781]

Meijer L, Raymond E. Roscovitine and other purines as kinase inhibitors. From starfish oocytes to clinical trials. Acc Chem Res 2003;36:417–25. [PubMed: 12809528]

Monaco EA 3rd, Beaman-Hall CM, Mathur A, Vallano ML. Roscovitine, olomoucine, purvalanol: inducers of apoptosis in maturing cerebellar granule neurons. Biochem Pharmacol 2004;67:1947–64. [PubMed: 15130771]

Mukhin AG, Ivanova SA, Allen JW, Faden AI. Mechanical injury to neuronal/glial cultures in microplates: role of NMDA receptors and pH in secondary neuronal cell death. J Neurosci Res 1998;51:748–58. [PubMed: 9545088]

Newcomb EW. Flavopiridol: pleiotropic biological effects enhance its anti-cancer activity. Anticancer Drugs 2004;15:411–9. [PubMed: 15166614]

Nguyen MD, Mushynski WE, Julien JP. Cycling at the interface between neurodevelopment and neurodegeneration. Cell Death Differ 2002;9:1294–306. [PubMed: 12478466]

Nguyen MD, Boudreau M, Kriz J, Couillard-Despres S, Kaplan DR, Julien JP. Cell cycle regulators in the neuronal death pathway of amyotrophic lateral sclerosis caused by mutant superoxide dismutase 1. J Neurosci 2003;23:2131–40. [PubMed: 12657672]

Okamoto T, Yamamura K, Hino O. The mouse interferon-gamma transgene chronic hepatitis model (Review). Int J Mol Med 1999;3:517–20. [PubMed: 10202184]

Park DS, Obeidat A, Giovanni A, Greene LA. Cell cycle regulators in neuronal death evoked by excitotoxic stress: implications for neurodegeneration and its treatment. Neurobiol Aging 2000;21:771–81. [PubMed: 11124421]

Rashidian J, Iyirhiaro G, Aleyasin H, Rios M, Vincent I, Callaghan S, Bland RJ, Slack RS, During MJ, Park DS. Multiple cyclin-dependent kinases signals are critical mediators of ischemia/hypoxic neuronal death in vitro and in vivo. Proc Natl Acad Sci U S A 2005;102:14080–5. [PubMed: 16166266]

Sakurai M, Hayashi T, Abe K, Itoyama Y, Tabayashi K, Rosenblum WI. Cyclin D1 and Cdk4 protein induction in motor neurons after transient spinal cord ischemia in rabbits. Stroke 2000;31:200–7. [PubMed: 10625738]

Seo HR, Lee DH, Lee HJ, Baek M, Bae S, Soh JW, Lee SJ, Kim J, Lee YS. Cyclin G1 overcomes radiation-induced G2 arrest and increases cell death through transcriptional activation of cyclin B1. Cell Death Differ 2006;13:1475–84. [PubMed: 16322753]

Silver J, Miller JH. Regeneration beyond the glial scar. Nat Rev Neurosci 2004;5:146–56. [PubMed: 14735117]

Sultana R, Butterfield DA. Regional expression of key cell cycle proteins in brain from subjects with amnestic mild cognitive impairment. Neurochem Res 2007;32:655–62. [PubMed: 17006763]

Takuma K, Baba A, Matsuda T. Astrocyte apoptosis: implications for neuroprotection. Prog Neurobiol 2004;72:111–27. [PubMed: 15063528]

Tamatani M, Che YH, Matsuzaki H, Ogawa S, Okado H, Miyake S, Mizuno T, Tohyama M. Tumor necrosis factor induces Bcl-2 and Bcl-x expression through NFkappaB activation in primary hippocampal neurons. J Biol Chem 1999;274:8531–8. [PubMed: 10085086]

Tian DS, Dong Q, Pan DJ, He Y, Yu ZY, Xie MJ, Wang W. Attenuation of astrogliosis by suppressing of microglial proliferation with the cell cycle inhibitor olomoucine in rat spinal cord injury model. Brain Res 2007;1154:206–14. [PubMed: 17482149]

Walther M, Kuklinski S, Pesheva P, Guntinas-Lichius O, Angelov DN, Neiss WF, Asou H, Probstmeier R. Galectin-3 is upregulated in microglial cells in response to ischemic brain lesions, but not to facial nerve axotomy. J Neurosci Res 2000;61:430–5. [PubMed: 10931529]

Wang F, Corbett D, Osuga H, Osuga S, Ikeda JE, Slack RS, Hogan MJ, Hakim AM, Park DS. Inhibition of cyclin-dependent kinases improves CA1 neuronal survival and behavioral performance after global ischemia in the rat. J Cereb Blood Flow Metab 2002;22:171–82. [PubMed: 11823715]

Yakovlev AG, Knoblach SM, Fan L, Fox GB, Goodnight R, Faden AI. Activation of CPP32-like caspases contributes to neuronal apoptosis and neurological dysfunction after traumatic brain injury. J Neurosci 1997;17:7415–24. [PubMed: 9295387]

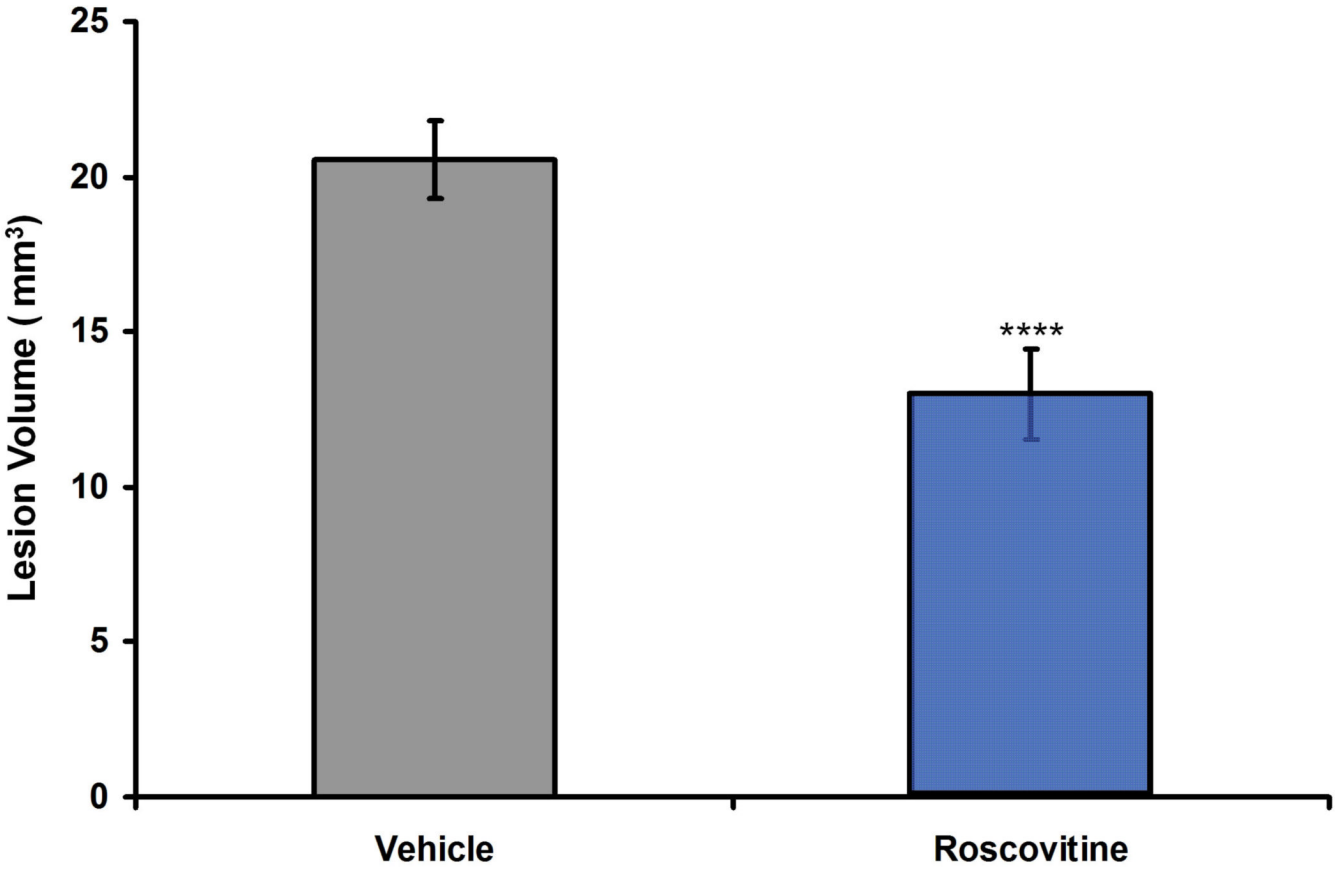

Fig. 1.
Treatment with roscovitine, 30 min following TBI, significantly decreases lesion volume. Lesion volume was measured 21 days following injury and compared to vehicle-treated animals (t=5.073, ****P<0.001; n=7-8 per group).

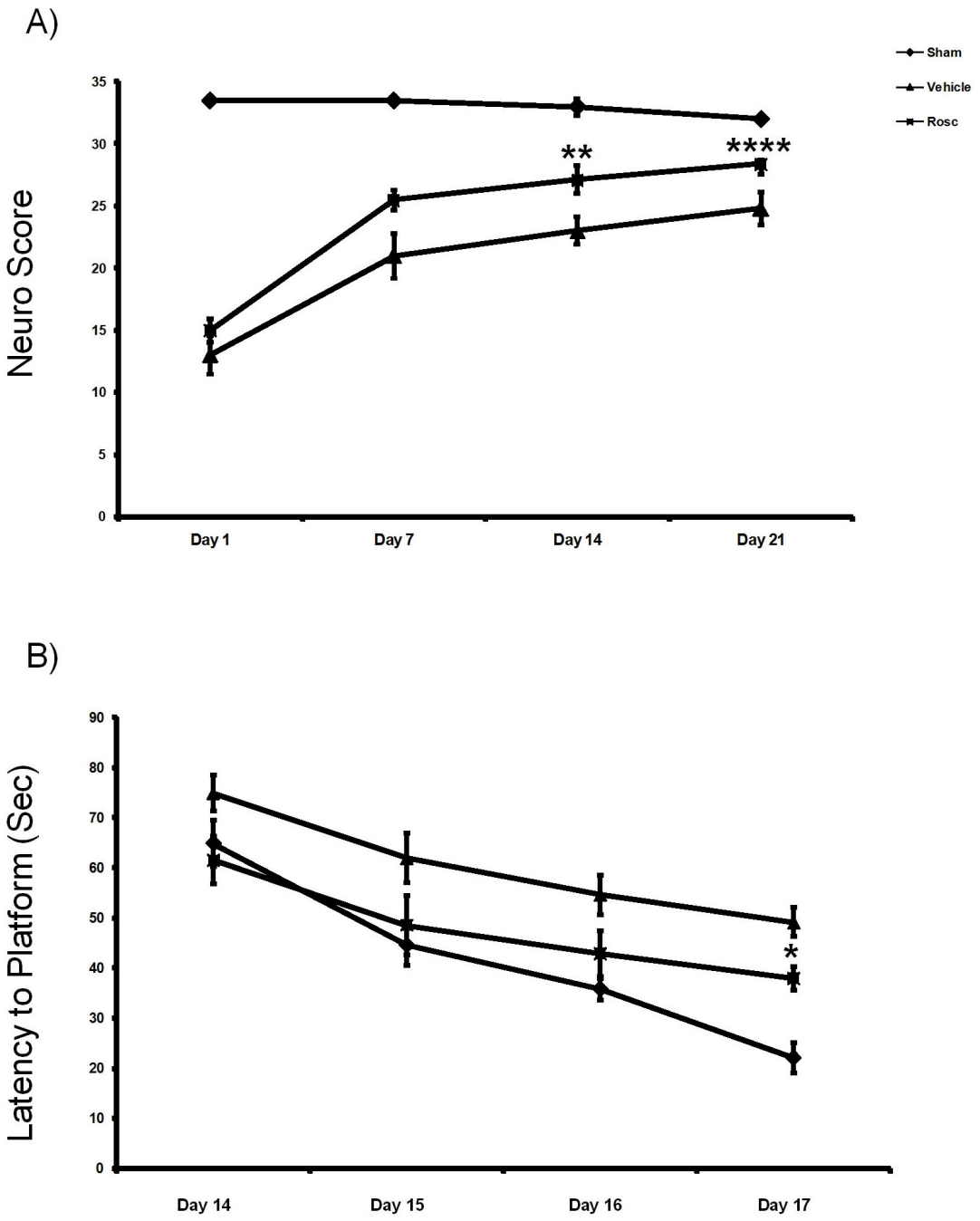

Fig. 2.

Administration of roscovitine significantly attenuates functional deficits induced by TBI. (A) Roscovitine improved motor function, as measured by the composite neuroscore at 14 and 21 days following injury (each n=7-8). Vehicle-treated injured animals show significantly lower neuroscores compared to sham animals at all time points ($P<0.005$); injured animals treated with roscovitine show improved motor function compared to vehicle-treated injured animals at 14 day (**$P<0.02$) and 21 days (****$P<0.001$) after injury. (B) Treatment with roscovitine significantly improves performance on the Morris water maze. Vehicle-treated injured animals demonstrate a significantly longer latency to platform compared to sham animals by 16 ($P<0.05$) and 17 ($P<0.001$) days post-injury. Injured animals treated with roscovitine had a

significantly shorter latency to platform by 17 days after injury compared to vehicle-treated injured animals (*P<0.05).

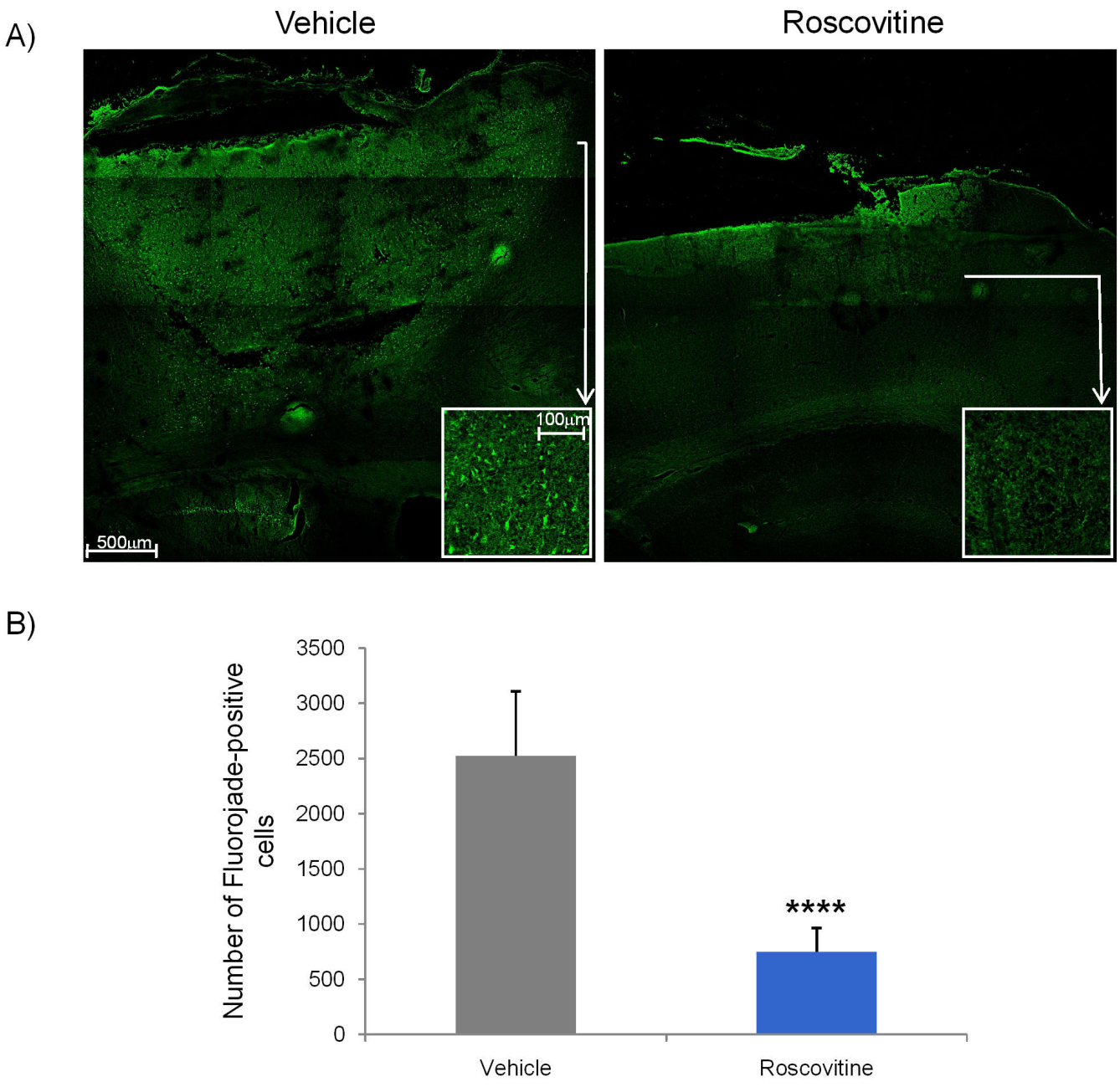

Fig. 3.

Roscovitine treatment decreases neuronal cell death as indicated by Fluoro Jade C staining 24 h after injury. (A) Vehicle-treated animals demonstrate a large lesion injury containing many degenerating neurons (Fluoro Jade C positive) whereas the roscovitine-treated animals showed a decreased lesion area and fewer Fluoro Jade C positive neurons. The image insets are generated from the same file as the main confocal image and present at higher magnification an area from the indicated region. (B) Cell counting using ImageJ indicates that roscovitine treatment results in a significant decrease in Fluro Jade-positive cells per brain section (n=4 sections, threshold=50, unpaired t test, **** P=0.0004).

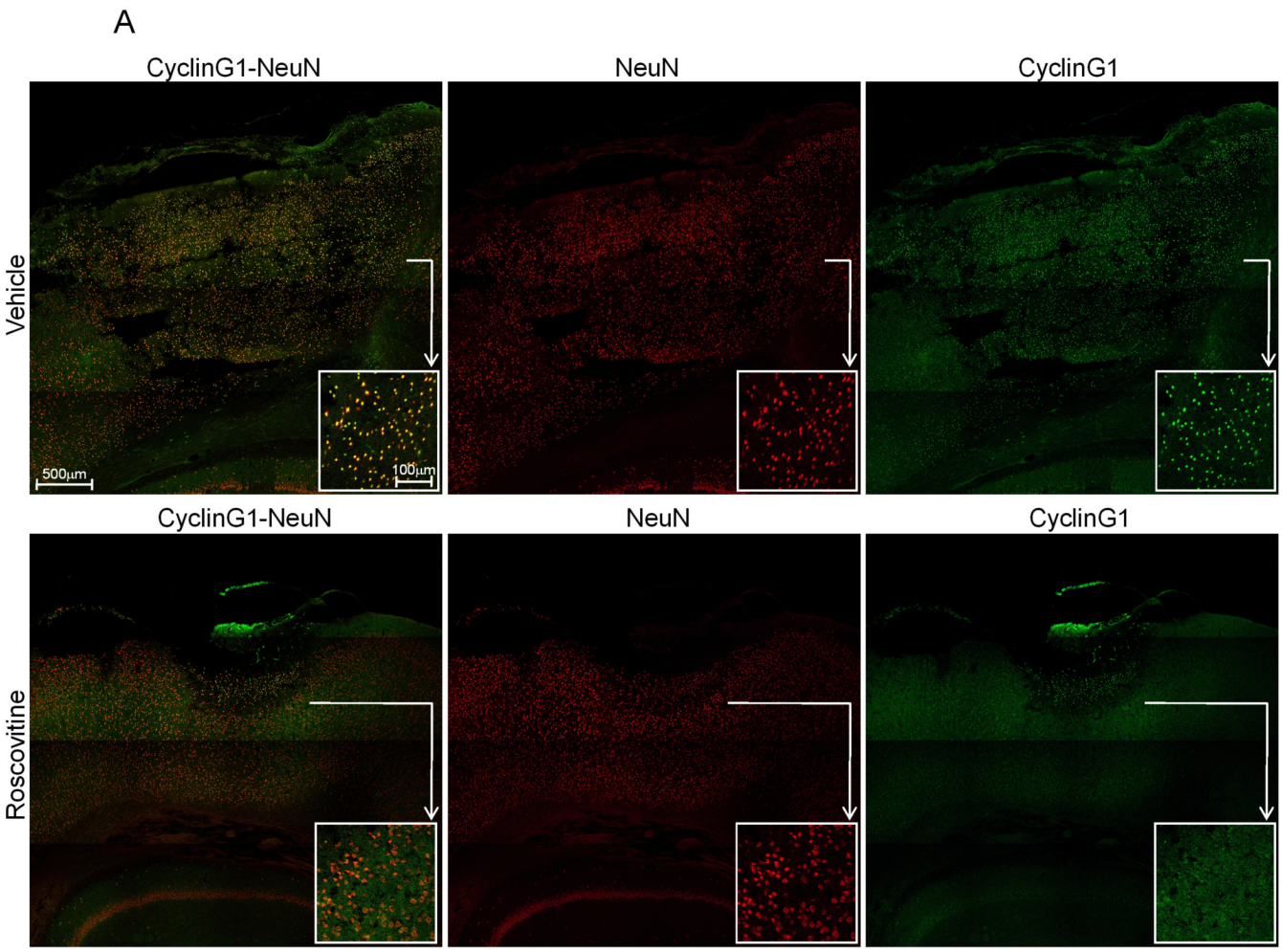

B

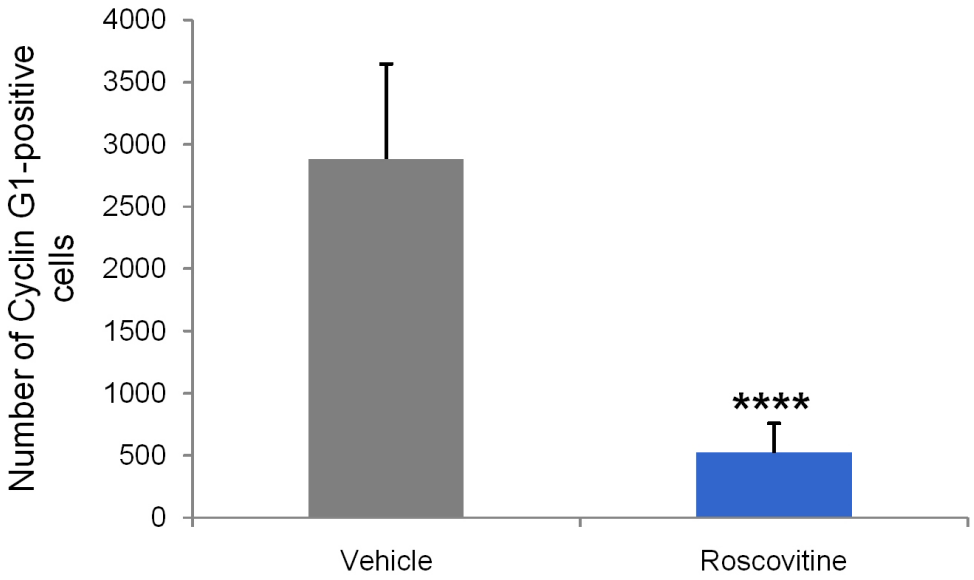

C

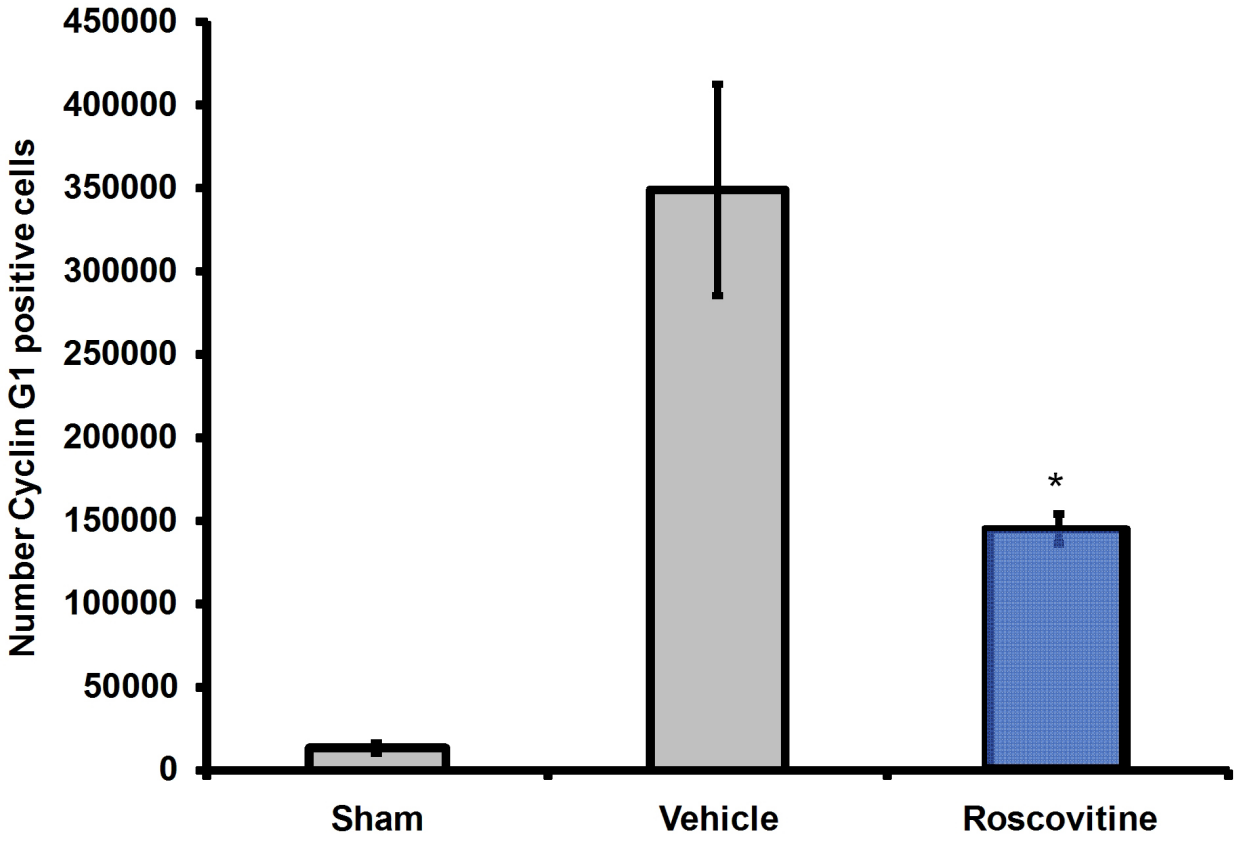

Fig. 4.

Roscovitine treatment significantly decreases expression of Cyclin G1 in neurons 24 h after injury. (A) Representative composite confocal images after double-immunostaining for cyclin G1 (green) and NeuN, neurons-specific antigen (red) of the lesion injury show the decrease in the number of neurons positive for cyclin G1 immunostaining (colocalization indicated yellow color) in roscovitine compared to vehicle. The separate NeuN and cyclin G1 images are also shown for both vehicle- and roscovitine-treated animals, respectively. The image insets are generated from the same file as the main confocal image and present at higher magnification an area from the indicated region. (B) Cell counting using ImageJ indicates that roscovitine treatment results in a significant decrease in Cyclin G1-positive cells per brain section (n=5 sections, threshold=99, unpaired t test, **** P=0.0002). (C) Quantitative assessment using stereology demonstrates that injury increases expression of Cyclin G1 compared to sham-treated animals (P<0.02), and that roscovitine treatment significantly decreased the number of cyclin G1 positive cells compared to vehicle (n=3-4; *P<0.05), although not to levels observed in sham animals (P<0.05).

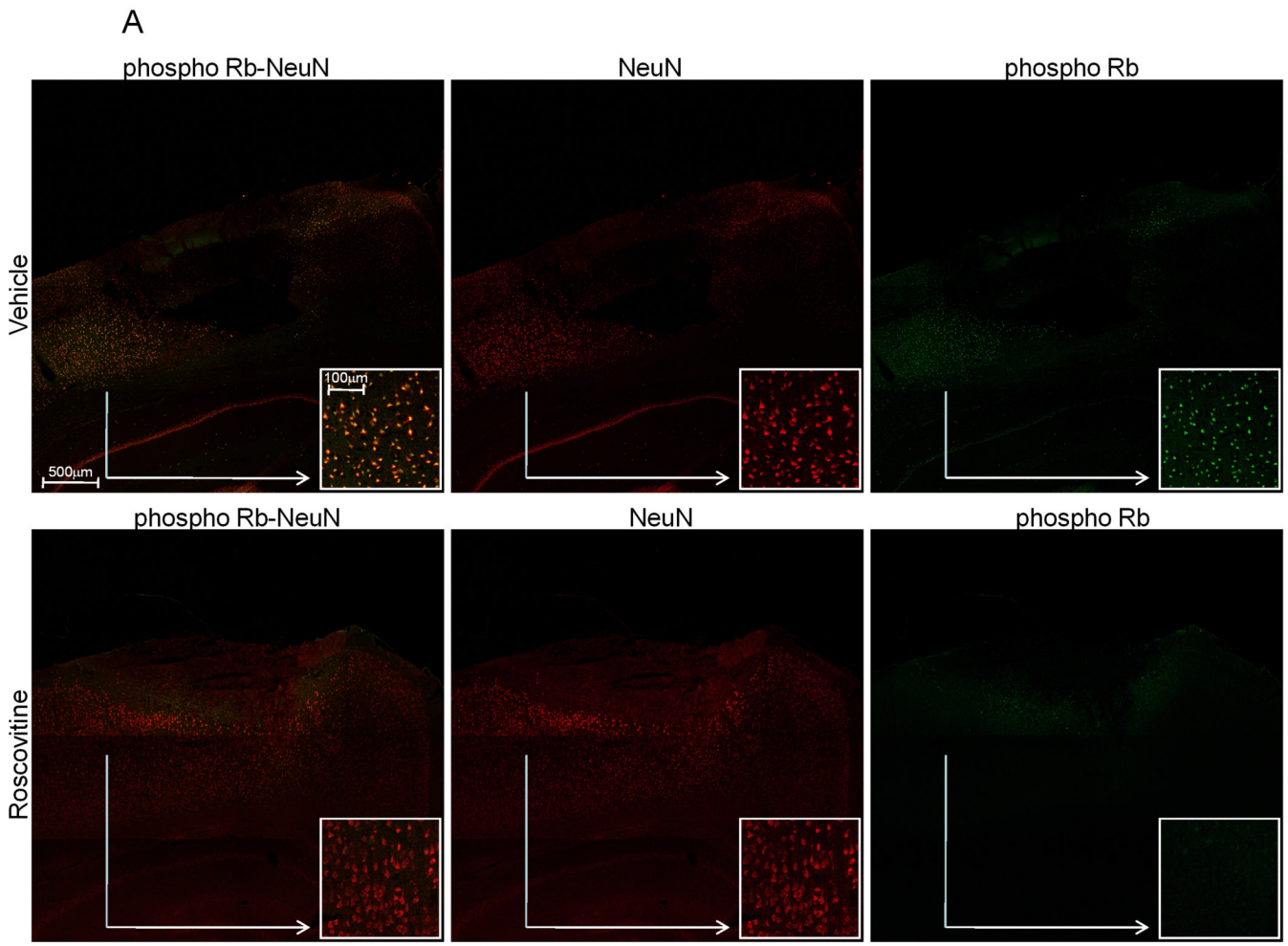

B

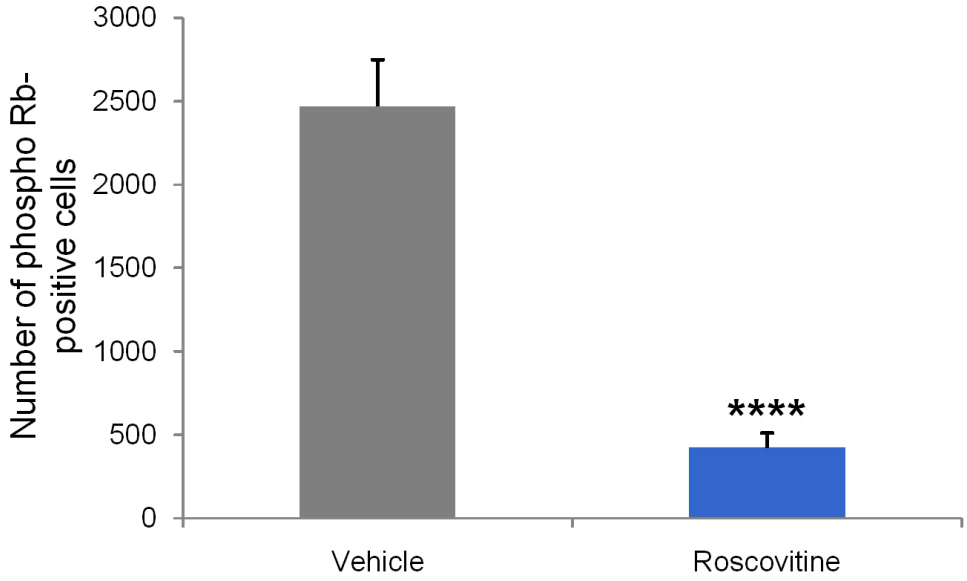

C

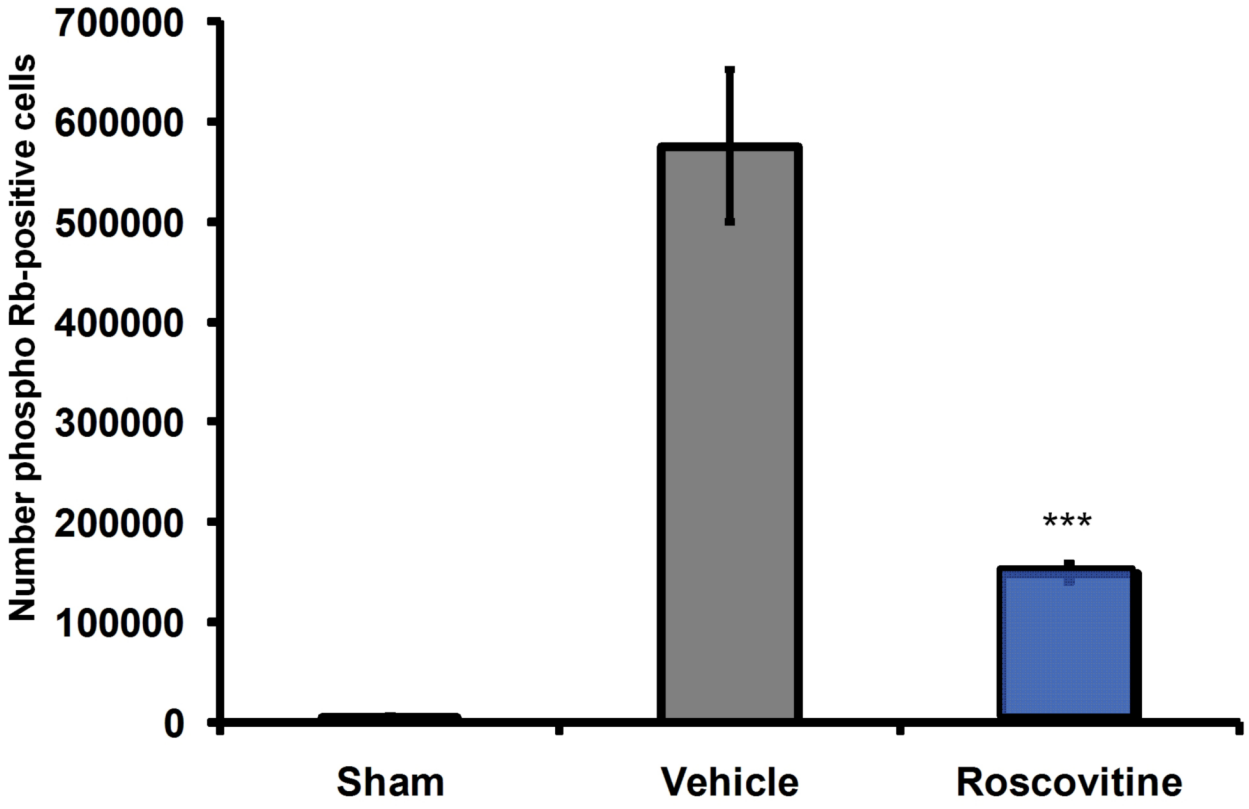

Fig. 5.

Roscovitine treatment significantly attenuates the phosphorylation of Rb in neurons 24 h after injury. (A) Representative composite confocal images after double-immunostaining for phospho-Rb (green) and NeuN, neurons-specific antigen (red) of the lesion injury show the decrease in the number of neurons positive for phospho-Rb immunostaining (colocalization indicated yellow color) in roscovitine compared to vehicle. The separate NeuN and phospho-Rb images are also shown for both vehicle- and roscovitine-treated animals, respectively. The image insets are generated from the same file as the main confocal image and present at higher magnification an area from the indicated region. (B) Cell counting using ImageJ indicates that roscovitine treatment results in a significant decrease in phospho-Rb-positive cells per brain section (n=4 sections, threshold=29, unpaired t test, **** $P<0.0001$) (C) Quantitative assessment using stereology demonstrates that injury increases phosphorylated Rb compared to sham ($F_{2,10} = 27.386$, $P<0.001$) and treatment with roscovitine significantly decreases the number of phospho-Rb positive cells compared to vehicle (***$P<0.002$).

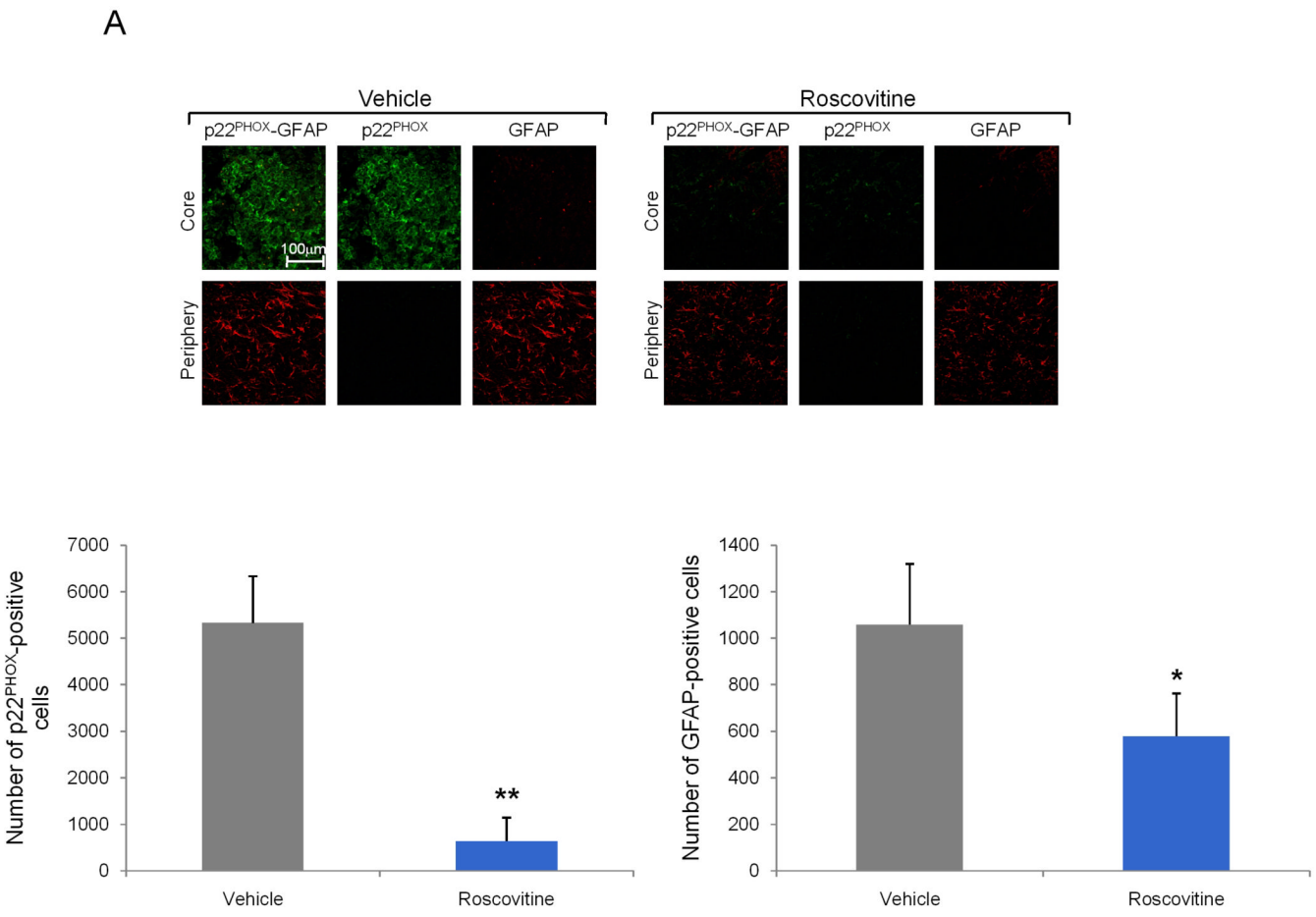

B

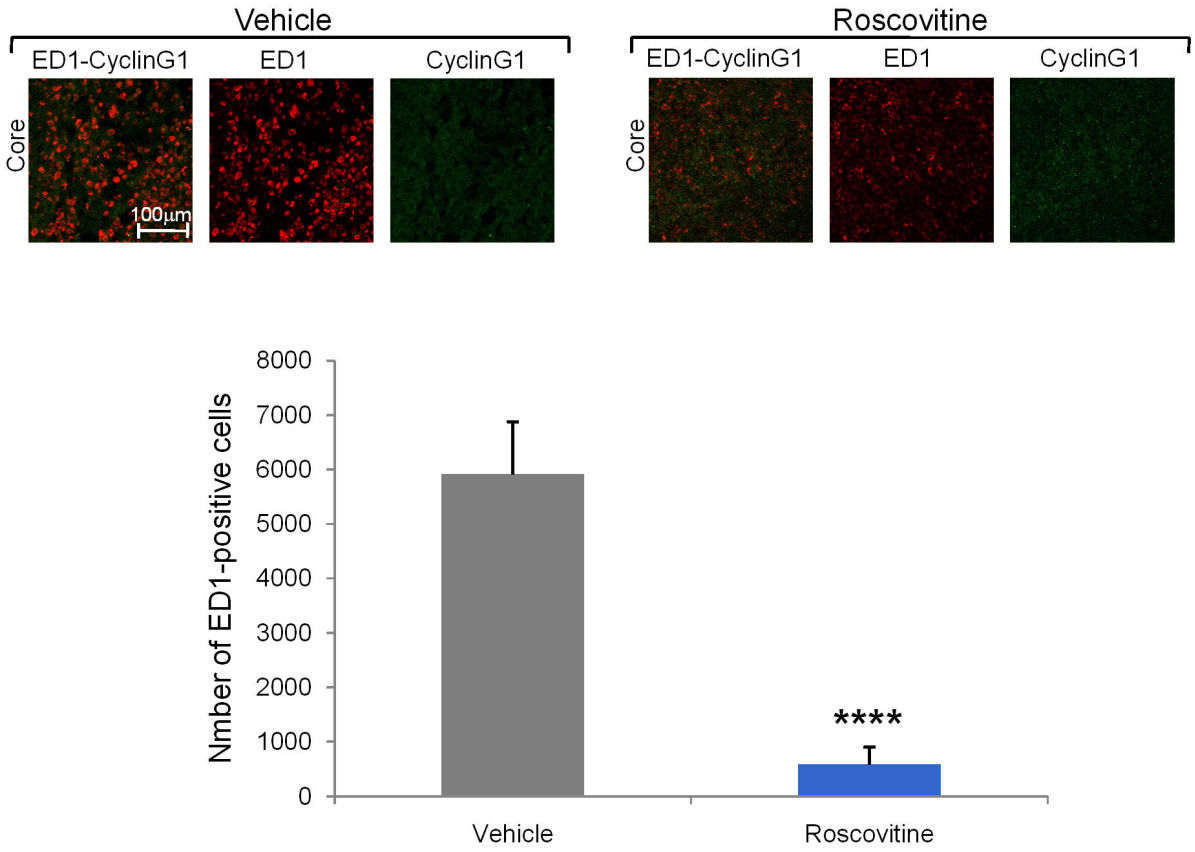

C

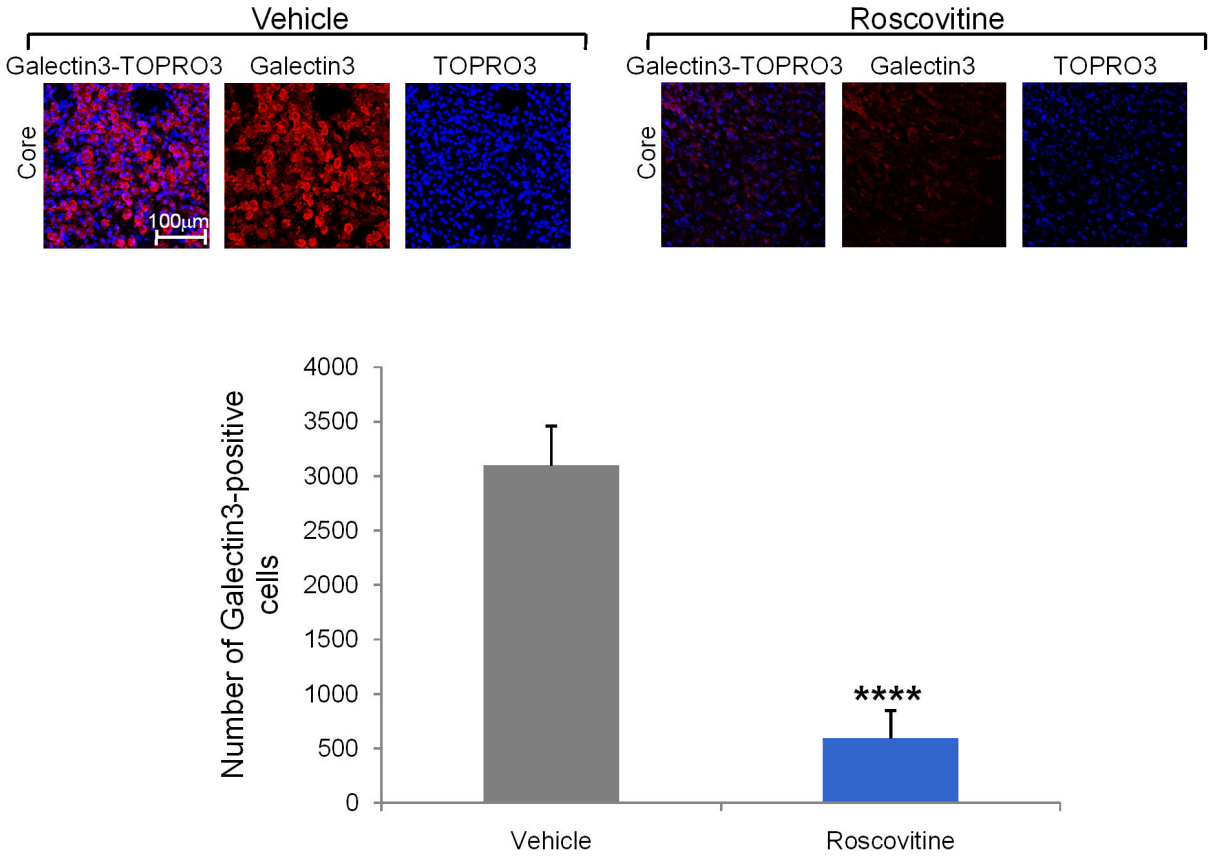

D

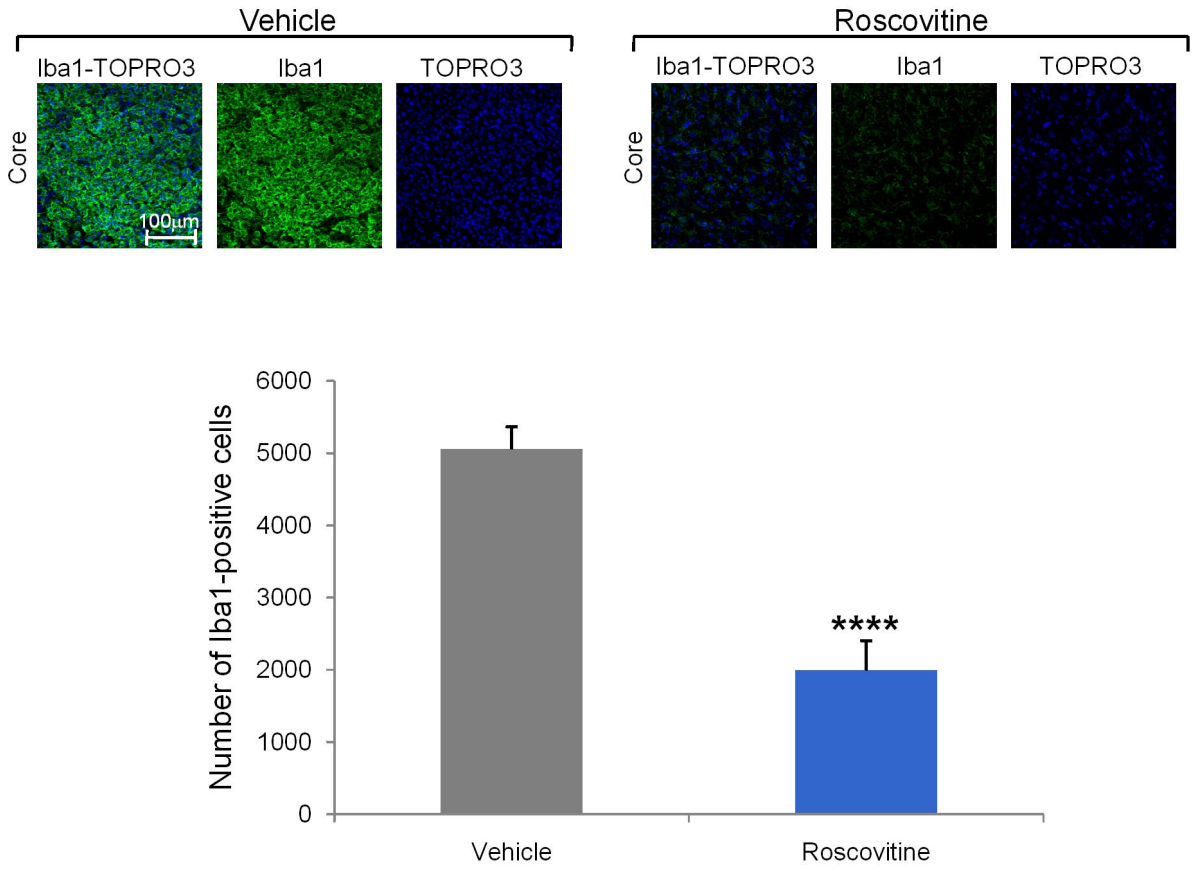

Fig. 6.

Roscovitine treatment decreases activation of microglial and astroglia at 7 days after injury, as indicated by immunostaining for $p22^{PHOX}$, ED1, Galectin-3 and GFAP. All images are cropped from the indicated areas of larger multi-tile images (data not shown); multi-tile images are used for the cell counting data presented. (A) Representative composite confocal images after double-immunostaining for GFAP (red) and $p22^{PHOX}$ (green) of the core and periphery of the injury show that injury-dependent increase in the number of $p22^{PHOX}$-positive microglia is concentrated in the core, whereas the increase in GFAP-positive astroglia, occurs especially in the periphery of the lesion. Roscovitine attenuated both changes. There is no colocalization between markers for microglia and astroglia. Images showing the separate $p22^{PHOX}$ and GFAP channels are included. Cell counting using ImageJ indicates that roscovitine treatment results in a significant decrease in both $p22^{PHOX}$ (n=3 sections, threshold=50, unpaired t test, ** P=0.0029) and GFAP-positive cells (n=3 sections, threshold=150, unpaired t test, * P=0.0298) per brain section. (B) Representative composite confocal images after double-immunostaining for ED1 (red) and cyclin G1 (green) of the injury core show the increased number of ED1-positive microglia after TBI. These cells do not have increased cyclin G1 staining. Roscovitine

treatment attenuated the ED1 staining increase. There is no colocalization between ED1 and cyclin G1 immunostaining. Images with separate ED1 and cyclin G1 channels are also shown for both vehicle- and roscovitine-treated animals, respectively. Cell counting using ImageJ indicates that roscovitine treatment results in a significant decrease in ED1-positive cells (n=3 sections, threshold=50, unpaired t test, **** $P<0.0001$) per brain section. (C) Representative composite confocal images after immunostaining for Galectin-3 (red) and staining with TO-PRO-3 (blue, DNA stain) of the area of the injury core illustates the increased number of Galectin-3-positive microglia. Roscovitine treatment attenuated the increased Galectin-3 staining. The separate Galectin-3 and TO-PRO-3 images are also shown for both vehicle- and roscovitine-treated animals, respectively. Cell counting using ImageJ indicates that roscovitine treatment results in a significant decrease in Galectin-3-positive cells (n=4 sections, threshold=50, unpaired t test, **** $P<0.0001$) per brain section. (D) Representative composite confocal images after immunostaining for Iba-1 (green) and staining with TO-PRO-3 (blue, DNA stain) of the area of the injury core illustates the increased number of Iba-positive microglia. Roscovitine treatment attenuated the increased Iba-1 staining. The separate Iba-1 and TO-PRO-3 images are also shown for both vehicle- and roscovitine-treated animals, respectively. Cell counting using ImageJ indicates that roscovitine treatment results in a significant decrease in Iba-1-positive cells (n=4 sections, threshold=50, unpaired t test, **** $P<0.0001$) per brain section.

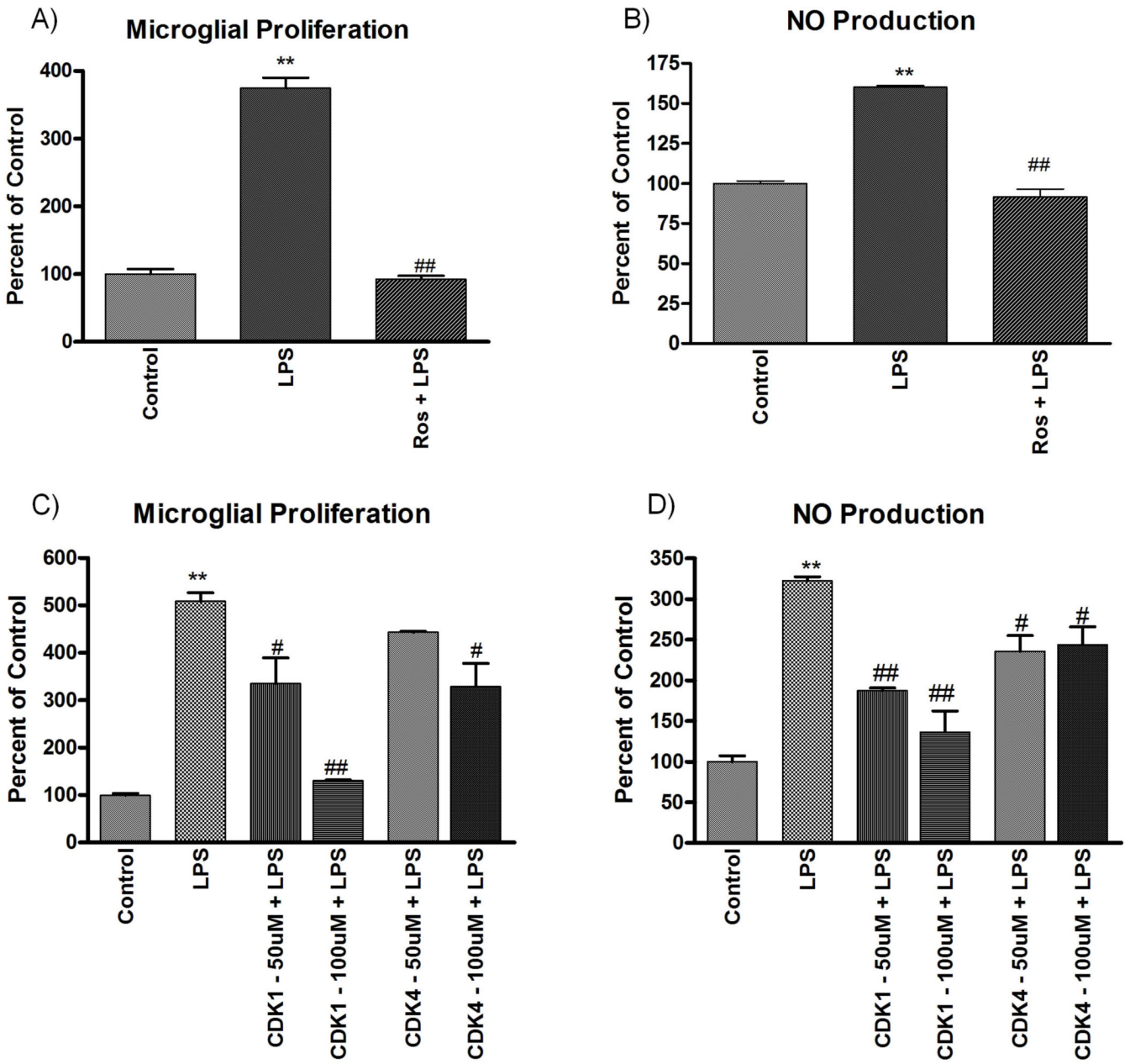

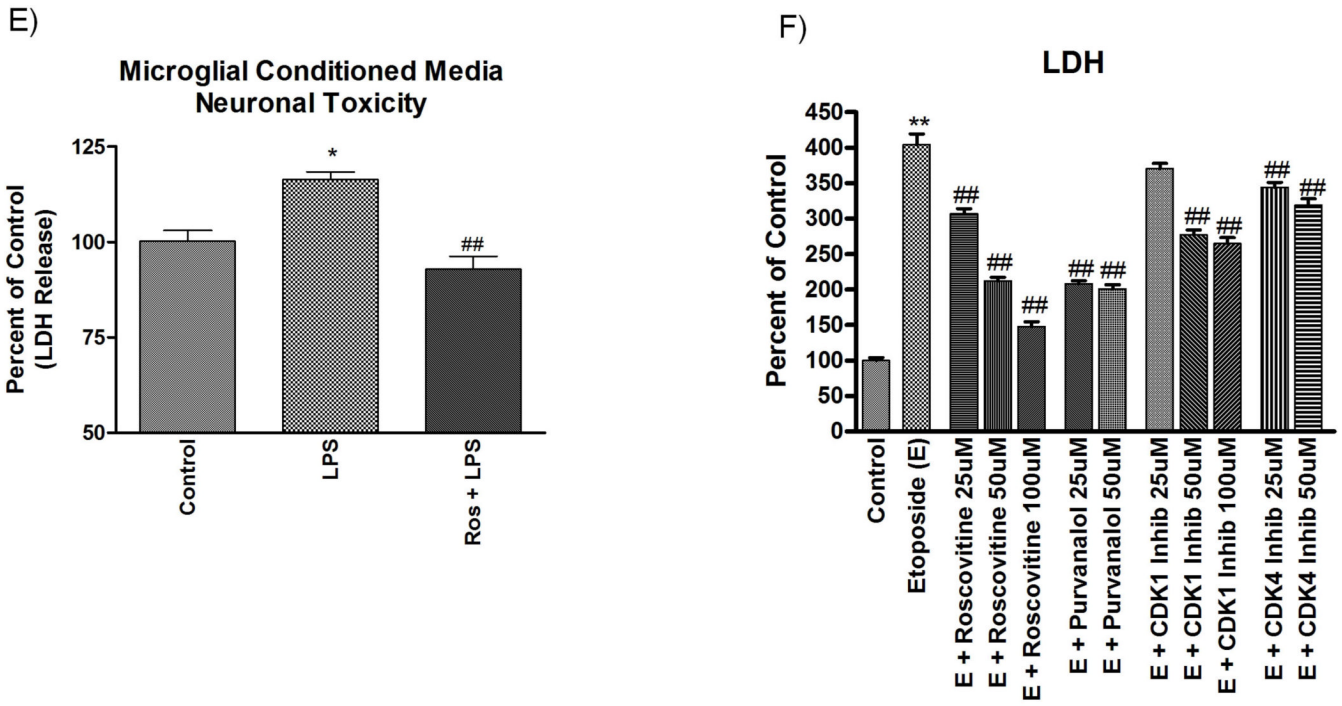

Fig. 7.

Roscovitine reduces activation of primary microglia and primary neuronal cell death in *in vitro* culture models. Primary rat microglia were incubated with LPS (1μg/ml) for 24 h and activation was determined by proliferation assays (A, C), release of NO (B, D) as well as neurotoxicity assays (F). Microglial proliferation was assessed using the MTS assay. Stimulation of primary microglial cultures with LPS (1μg/ml) for 24 h significantly increases microglial proliferation. Pre-treatment of microglia with roscovitine (Ros, 100μM) (A) or other CDK inhibitors at the indicated doses (B) for 1 h results in a significant attenuation of microglia proliferation. Bars represent mean +/- SEM; **P<0.001 in comparison to control; ##P<0.001 in comparison to LPS. Microglial activity was assessed by measuring the production of nitric oxide (NO) at 24 h after stimulation with LPS. Stimulation of primary microglial cultures with LPS significantly increases NO production. Pre-treatment of microglia with roscovitine (Ros, 100μM) (C) or other CDK inhibitors at the indicated doses (D) for 1 h results in a significant inhibition of NO production. Bars represent mean +/- SEM; **P<0.001 in comparison to control; ##P<0.001 in comparison to LPS. (E) To determine neurotoxicity, conditioned media from microglia stimulated for 24 h with LPS was transferred to primary rat neurons. After an additional 24 h, neuronal viability was assayed by measuring LDH release. Conditioned media from microglia pre-treated with roscovitine (100μM) for 1 h prior to LPS stimulation results in a complete inhibition of microglial-induced neuronal death. Bars represent mean +/- SEM; *P<0.05 in comparison to control; ##P<0.001 in comparison to LPS. (F) To determine neuroprotection, primary cortical neurons were pretreated with the indicated doses of roscovitine and other CDK inhibitors, then exposed to etoposide (50μM) for 24 h followed by determination of neuronal viability assayed by measuring LDH release. Roscovitine as well as the other CDK inhibitors resulted in significant attenuation of of etoposide-induced neuronal death. Bars represent mean +/- SEM; *P<0.05 in comparison to control; ##P<0.001 in comparison to etoposide alone.